Science Advances

AAAS

advances.sciencemag.org/cgi/content/full/3/1/e1600455/DC1

Supplementary Materials for

Marrow-inspired matrix cues rapidly affect early fate decisions of hematopoietic stem and progenitor cells

Ji Sun Choi and Brendan A. C. Harley

Published 6 January 2017, *Sci. Adv.* **3**, e1600455 (2017)
DOI: 10.1126/sciadv.1600455

This PDF file includes:

Supplementary Materials

Experimental design

Sample size. Sample size was chosen so that each data point would have values from at least three independent experiments (n = 3 or more) to compute statistically meaningful averages and standard deviations. Throughout our study, a sample refers to a HSC culture on a single hydrogel or glass substrate.

Rules for stopping data collection. We designed our experiments so that cultured cells would be analyzed at the end of the specified culture period (3-hrs or 24-hrs), at which point cells were either analyzed in situ or harvested and immediately treated for subsequent analyses. Freshly isolated cells were analyzed immediately following FACS. Data collection was stopped after performing at least three independent experiments for all of our planned experiments.

Data inclusion/exclusion criteria. Experimental conditions were chosen based on the findings from our previous publication (*25*). Originally, an expanded series of substrates (e.g., 227-kPa polyacrylamide gel substrates) were chosen as part of our experimental design. These substrates, however, appeared redundant as cell response was statistically indistinguishable from protein coated glass substrates (our stiff control substrate). We therefore narrowed our experimental polyacrylamide gel substrates to those with the stiffness of 3.7 kPa and 44 kPa to represent the stiffness associated with the bone marrow cavity and the endosteum.

Outliers. No data points generated from our experiments were excluded as outliers.

Selection of endpoints. An endpoint of 24-hr culture time was chosen based on our previous publication (*25*) which found that 24-hour culture period is sufficient to elicit HSC response in vitro. An endpoint of 3-hr culture time was chosen to illustrate HSC fate decisions occur rapidly once they are exposed to substrates resembling different microenvironmental conditions ex vivo.

Replicates. Because we utilized FACS-isolated primary HSCs whose numbers fluctuate from mouse to mouse, certain data points ended up with more or less technical replicates than others (n = 1-7).

Research objectives. Our previous findings (*25*) indicated that substrate stiffness and ligand density cause morphological changes in HSPC cultures. Recent reports in the literature have also linked HSC localization to disparate matrix environments ('niche') within the bone marrow. We therefore hypothesized that bone marrow niche associated characteristics (matrix stiffness and ligand, reflected in a series of culture substrates we fabricated) would differentially influence HSC fate decisions.

Research subjects or units of investigation. N/A.

Experimental design. All experiments were performed in a controlled laboratory environment. For all our experiments, we isolated and cultured primary murine HSCs on substrates pre-fabricated to exhibit combinations of matrix stiffness and ligands. Culture times (freshly isolated, 3-hour, 24-hour), substrate conditions (stiffness: 3.7 kPa, 44 kPa, 70 GPa (glass); ligand types: fibronectin or fibronectin analog (RGDfK), type I collagen, laminin), and treatment conditions (Blebbistatin, Y-27632, anti-$\alpha 5\beta 1$ or anti-$\alpha v\beta 3$ treatment) were varied to assess the impact of substrate stiffness and ligand types on HSC fate decisions in vitro. Morphological changes, viability, proliferation, and myeloid lineage specification of cultured cells were quantified using phase contrast imaging, Live/Dead assay, CellTrace™ Violet cell proliferation kit, and colony-forming unit assay, respectively.

Randomization and *Blinding.* N/A.

Cell viability quantification

HSC viability was assessed at the end of the 24h culture using Live/Dead Cell Viability Assay (Life Technologies, Grand Island, NY). Each sample was imaged at a minimum of 5 locations using an inverted fluorescence microscope (DMI4000, Leica Microsystems, Germany). The relative numbers of live (calcein positive, green) vs. dead (ethidium homodimer-1, red) cells were averaged to determine % viable cells among those that remained attached to the substrates.

Mechanical characterization of PA gels

The elastic moduli of PA gels were determined via atomic force microscopy (AFM; MFP-3D, Asylum Research Santa Barbara, CA) in a manner similar to previously described (*25*, *57*, *58*). In

summary, fully hydrated PA gel samples (n = 3-6) were probed in liquid contact mode to collect force indentation curves (n = 15-45), which were then analyzed to extract the elastic modulus. The elastic moduli of PA gel samples are summarized in **table S1**.

For mechanical characterization of PA gels via AFM, cantilever spring constant and optical lever sensitivity of the AFM were first calibrated against a glass slide (~70 GPa (*24*)) in ambient air contact mode. Then, deionized water droplet was placed on top of the glass slide and the sensitivity of the optical path was re-calibrated in liquid contact mode. Next, a PA gel sample fully immersed in deionized water was mounted. A silicon nitride probe with a pyramidal tip and a nominal spring constant of 0.06 N/m (Bruker Corp., Camarillo, CA) was used to collect force-indentation profiles with an indentation depth and scan rate of 1-2 μm and 1-2 μm/s, respectively. Slower scan rates were chosen to minimize any viscous effects arising from probing in the liquid environment. Force curve data obtained from AFM indentations were analyzed with the Hertz cone model. Only the approach (forward indentation) curves of the force-indentation profiles were used for analysis because retraction curves often exhibit high degrees of adhesive forces near the contact point. The AFM tip-sample interactions can be described by Hooke's law, which relates the applied loading force (F) to the spring constant (k) and the deflection (d) of the cantilever. Since the cantilever deflection is equal to the position of the z piezo (z) minus the sample indentation (δ), Hooke's law can be written as follows

$$F = k \times d = k(z - \delta) \quad (1)$$

Meanwhile, Hertz cone model relates the applied loading force to the sample indentation by the following equation

$$F = \frac{2}{\pi}\delta^2 \tan\alpha \frac{E}{1-\nu^2} \quad (2)$$

E and ν are the Young's modulus and the Poisson ratio of the sample and α is the half-opening angle of the cone or the cantilever tip in this case. Poisson ratio of the PA gels was assumed to be 0.4, consistent with the published range of 0.3-0.5 for PA substrates (*59*).

To apply the Hertz cone model to the obtained force curves, contact point had to be estimated. An AFM force curve consists of the noncontact region and the contact region separated by the contact

point (z_0, d_0), which is the point when the cantilever tip first comes in contact with the sample (fig. S11). Accurate determination of the contact point is therefore crucial to define the contact region and the resulting range of analysis. Incorporating the contact point into equations *1* and *2* yields the following

$$z - z_0 = d - d_0 + \sqrt{\frac{k(d-d_0)}{\frac{2}{\pi}\tan\alpha\frac{E}{1-\nu^2}}} \quad (3)$$

Lin *et al.* summarized various strategies employed to determine the contact point (*60*). Visual inspection approach is the simplest available method but it generally provides a poor fit because the quality of the fit is not considered. We previously reported the Young's moduli of the PA gels we fabricated using this approach (*25*).

In this study, we used a simple extrapolation to estimate the contact point. First, the zero deflection d_0 was estimated by fitting a linear line over the noncontact region. Next, a portion of the contact region or the 'range of analysis' bound by (z_1, d_1) and (z_2, d_2) was selected (fig. S11). The range of analysis (*58*) defines the range of cantilever deflection values and therefore the range of applied forces where Hertz model is fitted to extract the Young's modulus. Setting the range of analysis allowed the z piezo position at the point of contact (z_0) to be estimated using equation *3*. Once the contact point (z_0, d_0) was determined, the AFM force data within the defined range of analysis was plotted as F vs. δ^2. As in equation *2*, the slope of this plot gives the Young's modulus (E) of the sample. As a default, the range of analysis of 10-30 nm was chosen for analysis because it provided a good fit over PA gels with a varying stiffness. To facilitate the processing of the large volume of the AFM force curve data, we wrote a Matlab code that computes the Young's modulus of the sample based on this approach.

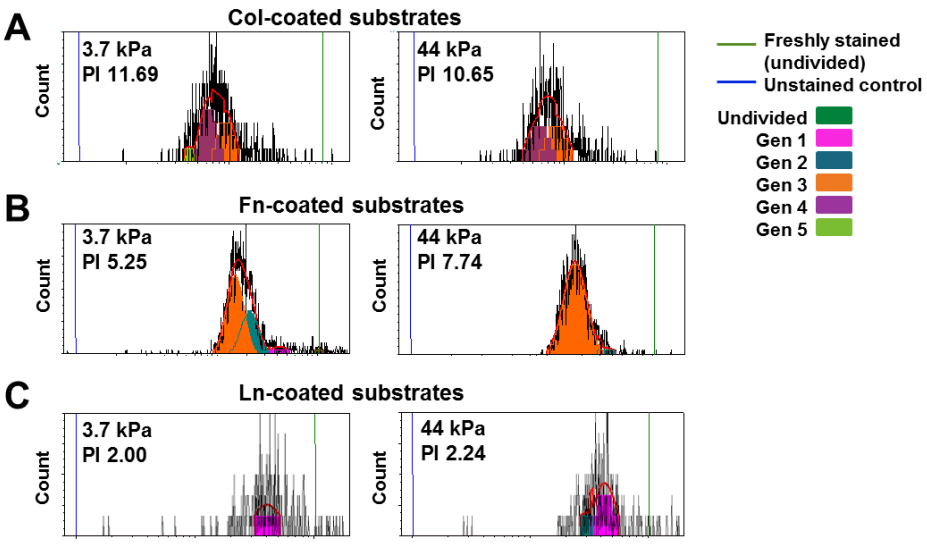

fig. S1. HSC proliferative index is increased on collagen substrates. After 24 hours of culture, HSCs were lifted with TripLE for proliferation analysis with CellTrace Violet. For this experiment, HSCs had been stained with CellTrace Violet stain prior to cell seeding. Lifted cells were analyzed with BD LSR II analyzer and flow data was analyzed with DeNovo FCS Express software. Representative images from data analysis are shown here for HSCs cultured on **(A)** collagen-coated, **(B)** fibronectin-coated, and **(C)** laminin-coated substrates.

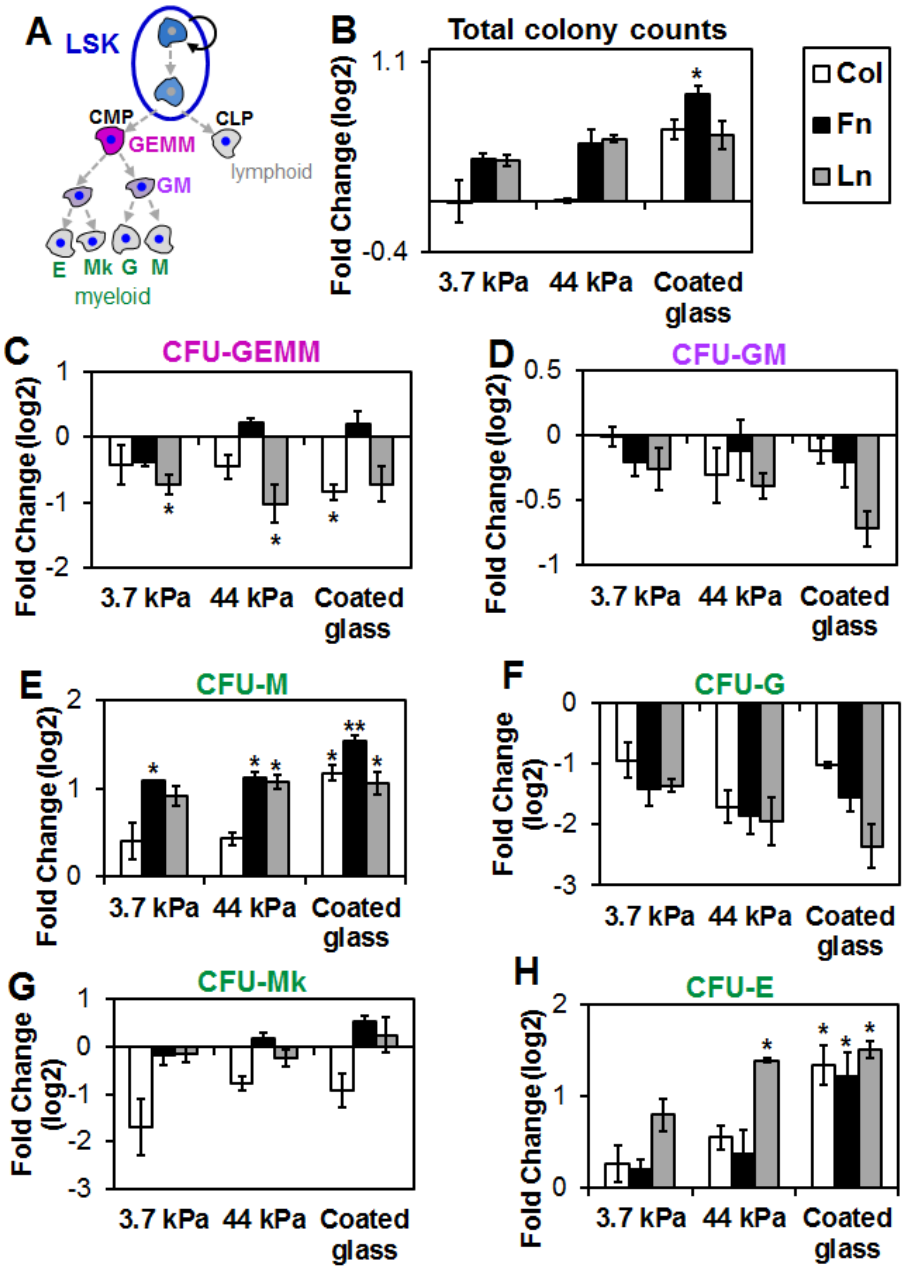

fig. S2. CFU colony counts of cultured HSCs compared to those from freshly isolated HSCs. **(A)** After 24 hours of culture, CFU assay was performed to assess myeloid lineage specification of the cultured HSCs. CMP, CLP, G, E, M, and Mk denote common myeloid progenitors, common lymphoid progenitors, and progenitors committed to granulocyte, erythrocyte, monocyte/macrophage, and megakaryocyte lineages, respectively. CFU colony numbers were then compared to those from freshly isolated HSCs to quantify the effect of matrix contact. The comparisons are summarized here as fold changes (log base 2) for **(B)** Total colony counts, **(C)** CFU-GEMM, **(D)** CFU-GM, **(E)** CFU-M, **(F)** CFU-G, **(G)** CFU-Mk, and **(H)** CFU-E from HSCs

cultured for 24 hours compared to those from freshly isolated HSCs. n = 3 from independent experiments. *: *p < 0.05. **: p < 0.001 with respect to CFU colonies that arose from freshly isolated HSCs.*

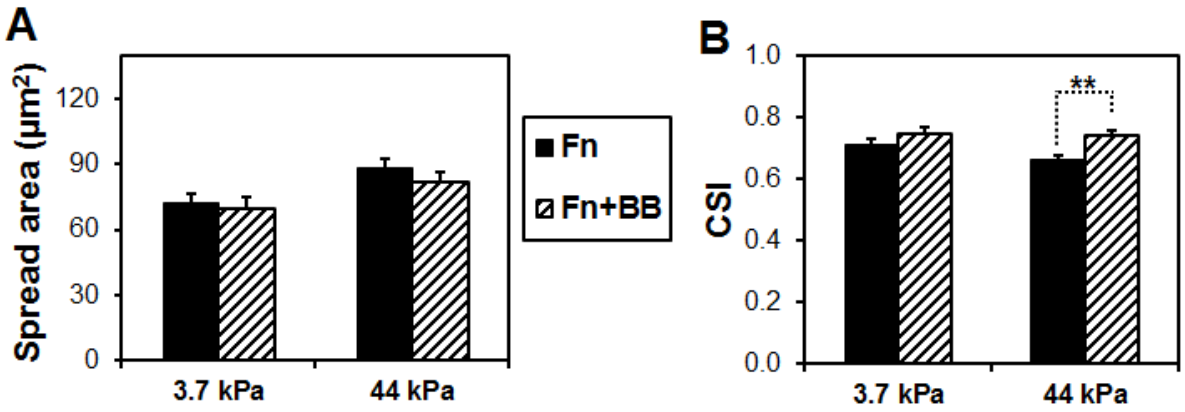

fig. S3. Morphology of cultured HSCs with blebbistatin added to the culture medium. HSCs were cultured for 24h with Blebbistatin (100 µM; "BB") added to the media. **(A)** Spread area and **(B)** Cell shape index (CSI) are shown. n = 29-35 cells. ***: p < 0.001*.

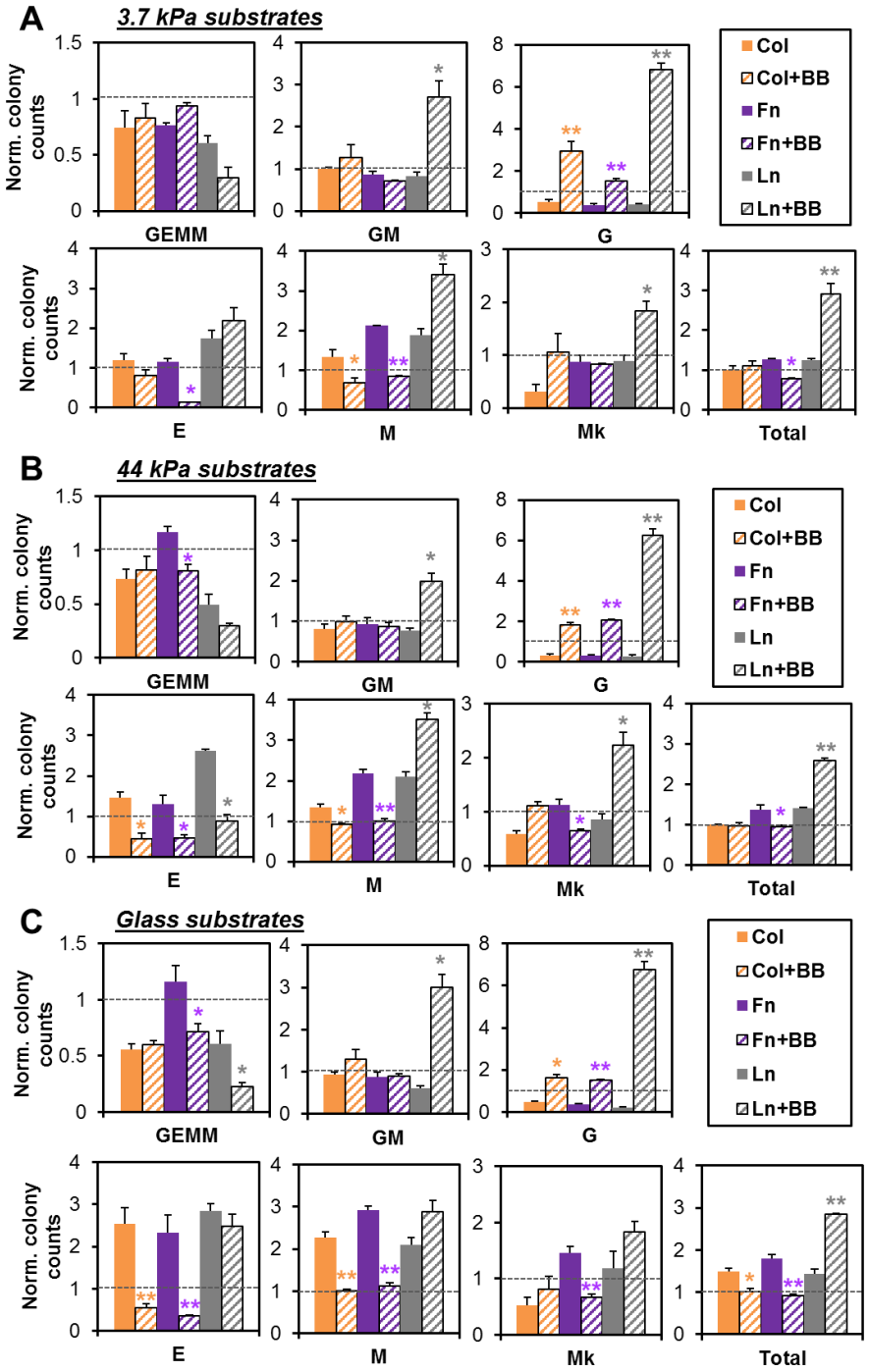

fig. S4. Actomyosin contractility alters HSC matrix engagement and lineage specification. Blebbistatin (100 μM, "BB") added to the culture media altered HSC response to matrix biophysical cues. CFU assay results (+/– BB) were normalized to colonies formed from a control group of freshly isolated HSCs (dashed lines). Normalized colony counts for HSCs cultured with and without BB on protein-coated **(A)** 3.7-kPa polyacrylamide gel, **(B)** 44-kPa polyacrylamide gel, and **(C)** glass substrates are shown. Blebbistatin abrogated previously noted stiffness-induced changes, with decreases in CFU-GEMM numbers on fibronectin-coated substrates and CFU-

E/M/Mk colonies on collagen- and fibronectin-coated substrates. A pronounced impact of matrix ligand cues was observed on later stage CFU colonies, with laminin substrates combined with BB promoting better myeloid specification compared to collagen or fibronectin. While matrix engagement reduced the number of CFU-G colonies for all matrix conditions, addition of Blebbistatin rescued CFU-G colonies, with a multiple-fold increase on laminin-coated substrates compared to collagen- or fibronectin-coated substrates. Col: Collagen. Fn: Fibronectin. Ln: Laminin. n = 3 from independent experiments. *: $p < 0.05$. **: $p < 0.001$.

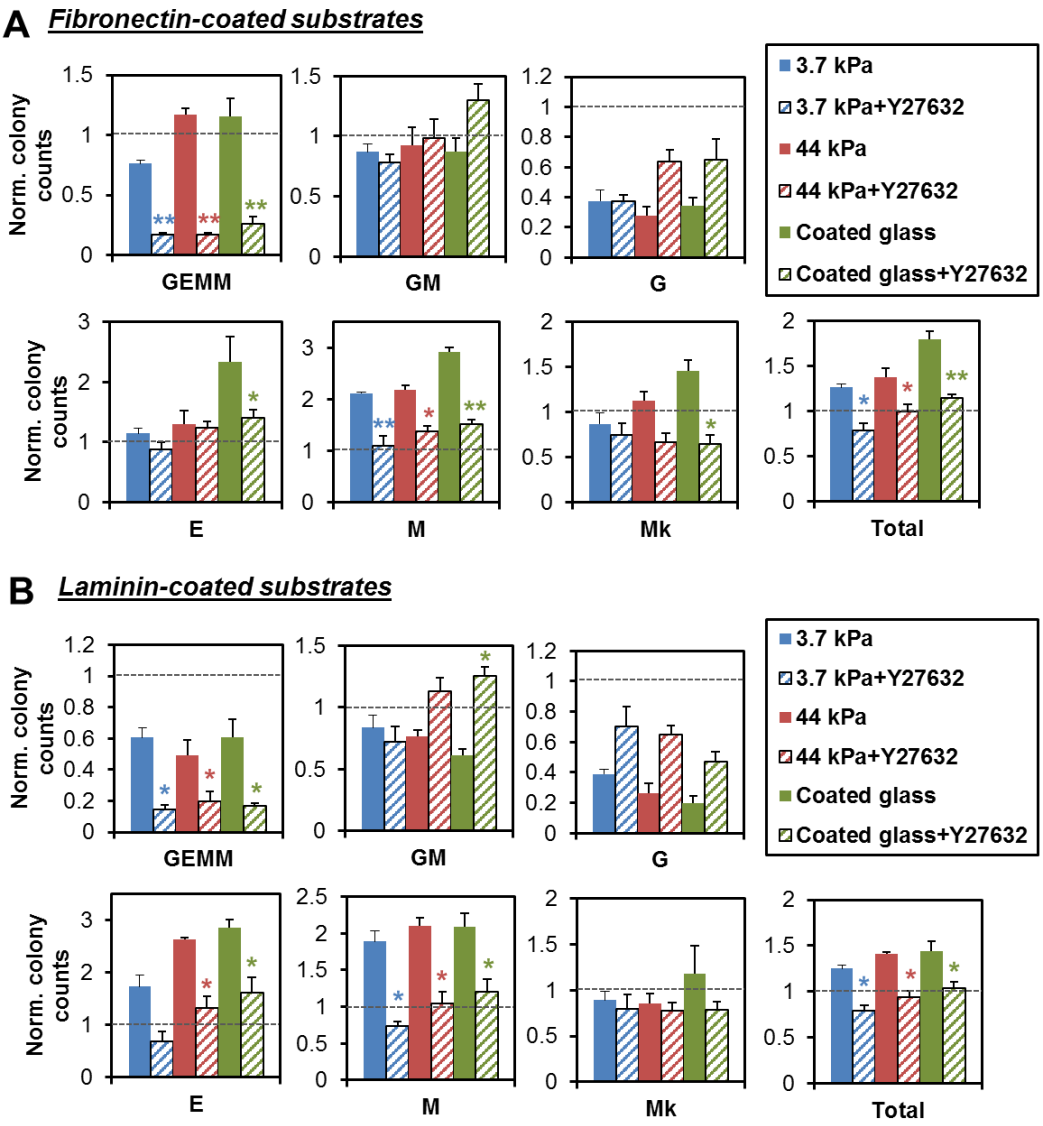

fig. S5. Myosin-mediated actin cytoskeletal tension alters HSC lineage specification. To assess the role of ROCK on myeloid lineage specification, primary HSCs were cultured with Y-27632 (10 μM), an inhibitor of ROCK known to modulate myosin activation and myosin-mediated actin cytoskeletal tension. After 24 hours, cultured cells were lifted and CFU assay was performed. All colony numbers were normalized to colonies from a control group of freshly isolated HSCs (dashed lines). Colony numbers from Y-27632 added samples are shown in stripes, next to colony numbers without Y-27632 shown as a comparison. Normalized colony counts from HSCs cultured on **(A)** fibronectin-coated and **(B)** laminin-coated substrates are shown. n = 4 from independent experiments. *: $p < 0.05$. **: $p < 0.001$.

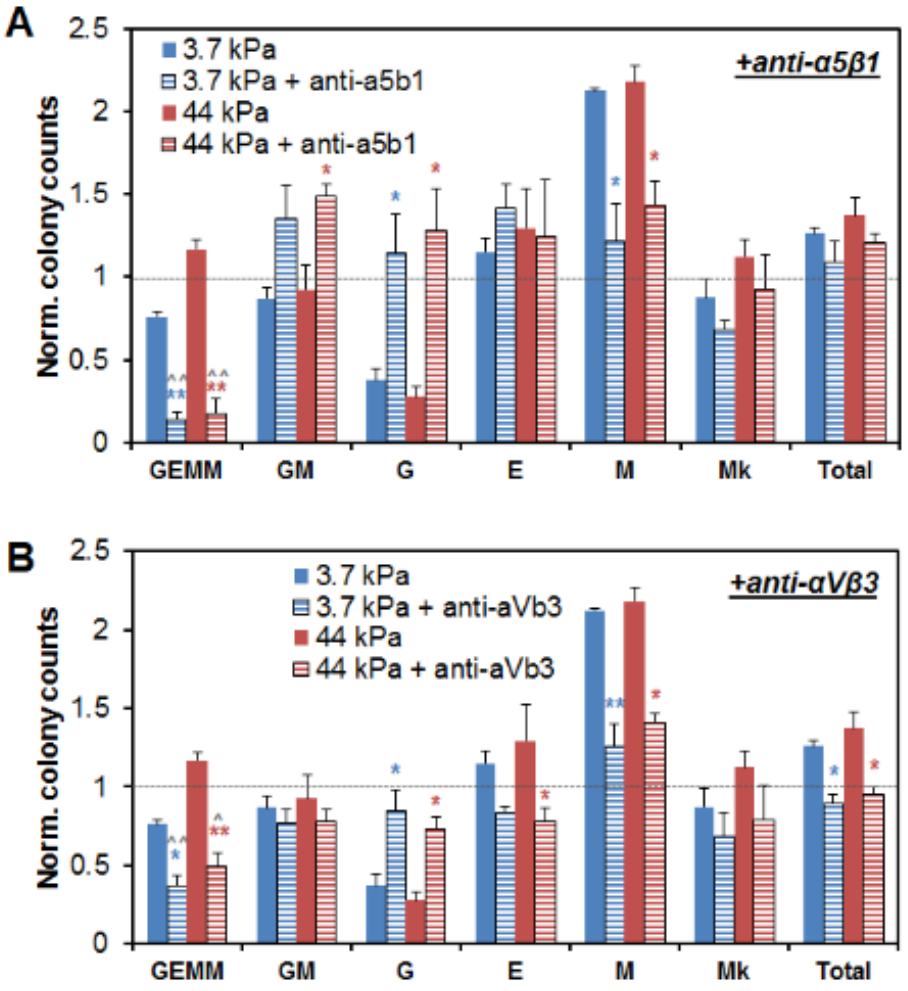

fig. S6. Role of integrins α5β1 and αvβ3 in myeloid lineage specification. To assess the role of specific integrin activation on myeloid lineage specification, **(A)** experimental substrates we treated with an antibody to α5β1 before seeding HSCs to inhibit binding to the RGD domain on fibronectin. Alternatively, **(B)** HSC binding to fibronectin was inhibited via treating experimental substrates with an antibody to αvβ3. Results here are compared to the conditions with no added antibodies, and reveal increased expansion of GM colonies and smaller decreases in GEMM colonies were observed on αvβ3 inhibited substrates. All colony numbers were normalized to those from freshly isolated HSCs, which are shown here as dashed lines at 1 (base level). n = 3-4. *: $p < 0.05$ and **: $p < 0.001$ with respect to no-antibody conditions. ^: $p < 0.05$ and ^^: $p < 0.001$ with respect to the base level.

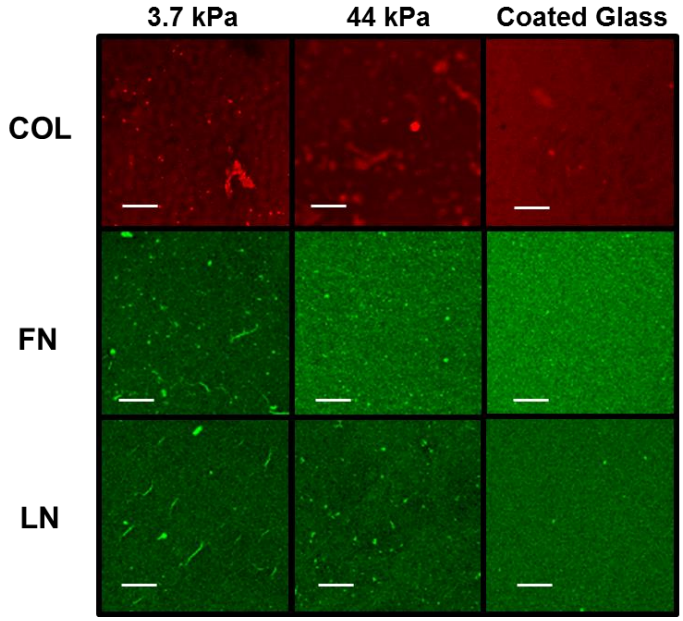

fig. S7. Immunofluorescence of protein-coated substrates. Visualizing the consistency of protein immobilization on experimental substrates using protein-coated substrates fluorescently tagged with appropriate primary and secondary antibodies (Alexa Fluor 564 or 488). COL: Collagen. FN: Fibronectin. LN: Laminin. Scale bar; 50 μm.

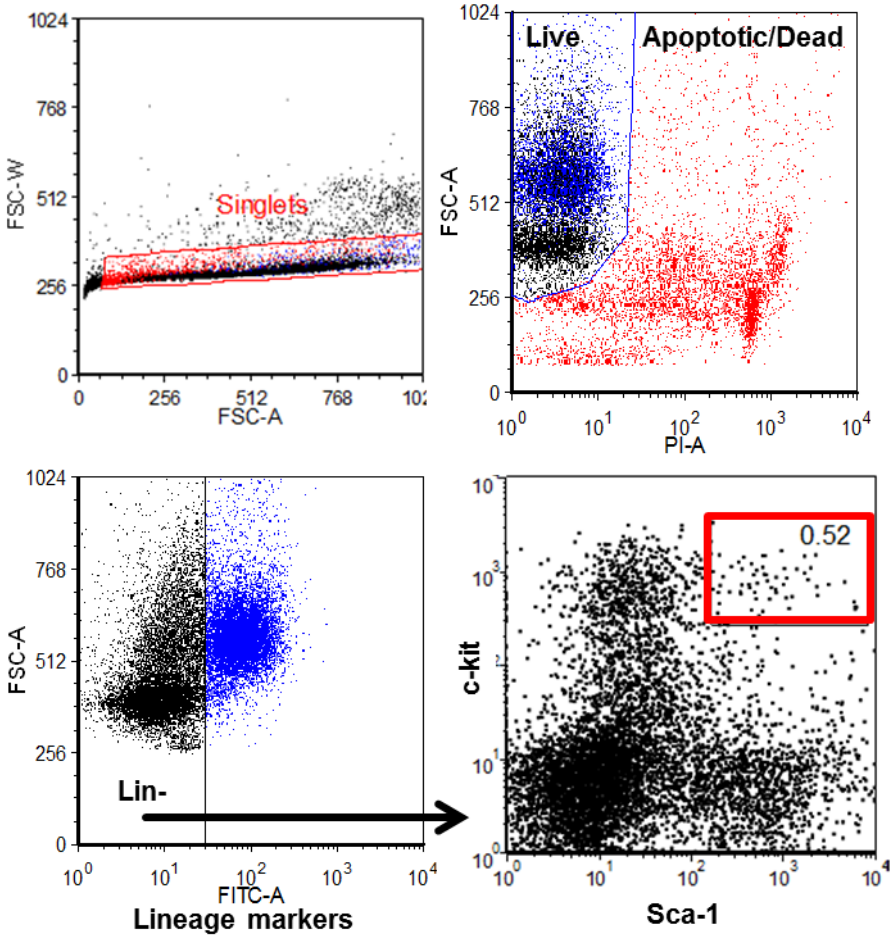

fig. S8. FACS isolation of LSK cell population. LSK (Lin $^{-}$Sca-1^{+}c-kit^{+}) cell population isolated from the marrow of murine femurs and tibias via FACS.

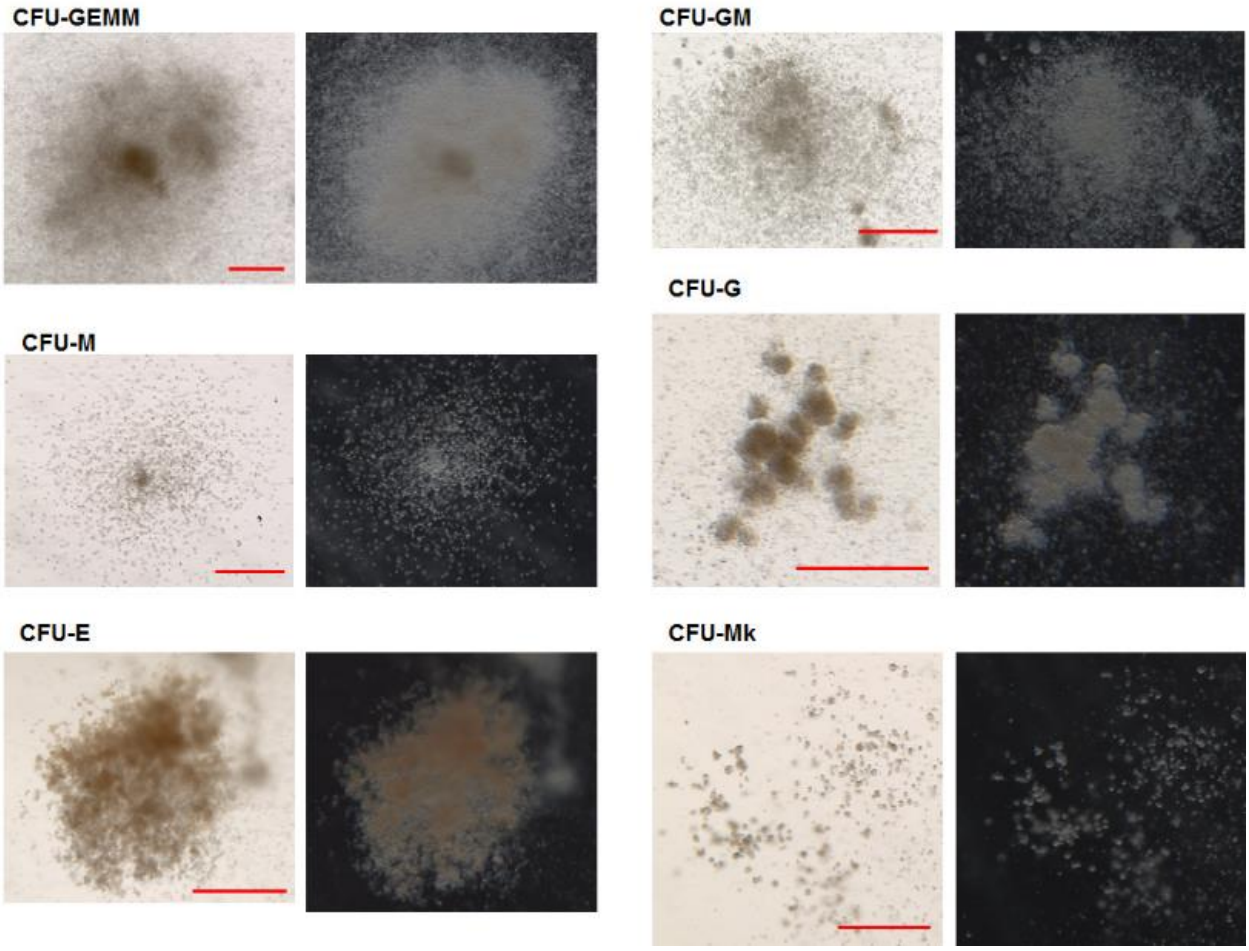

fig. S9. CFU colony enumeration. Cultured HSCs were lifted, resuspended in methylcellulose media, and incubated for 11-14 days for CFU colony enumeration. CFU-GEMM, CFU-GM, CFU-M, CFU-G, CFU-E, and CFU-Mk colonies were counted. Representative images of the colonies taken with Zeiss AxioZoom V16 microscope are shown here. Each brightfield image is accompanied by the corresponding darkfield image. Scale bars: 500 μm.

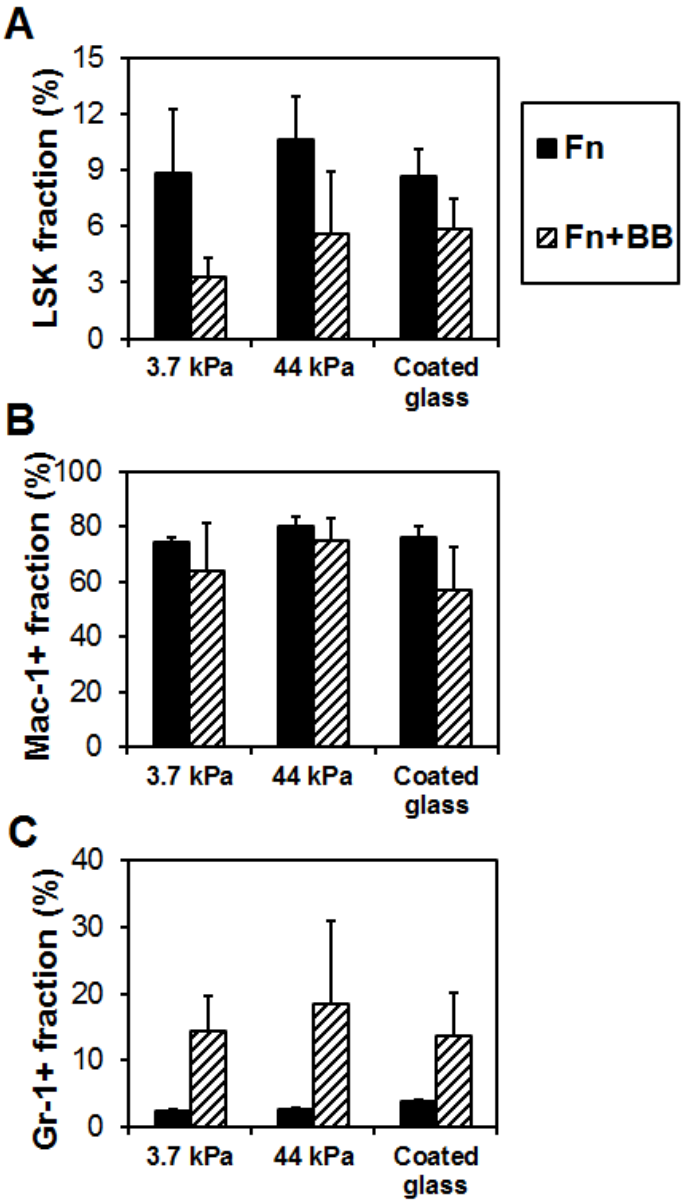

fig. S10. Flow cytometric analysis of the colony-forming cells harvested from the CFU assay. After colony enumeration, colony-forming cells from CFU-GEMM, CFU-M, and CFU-G colonies with or without Blebbistatin (+BB) on fibronectin-coated substrates were harvested from the methylcellulose media and stained for flow cytometric analysis. The percentage of cells that were **(A)** LSK, **(B)** Mac-1+, and **(C)** Gr-1+ from CFU-GEMM, CFU-M, and CFU-G, respectively, are shown. n = 3 from independent experiments.

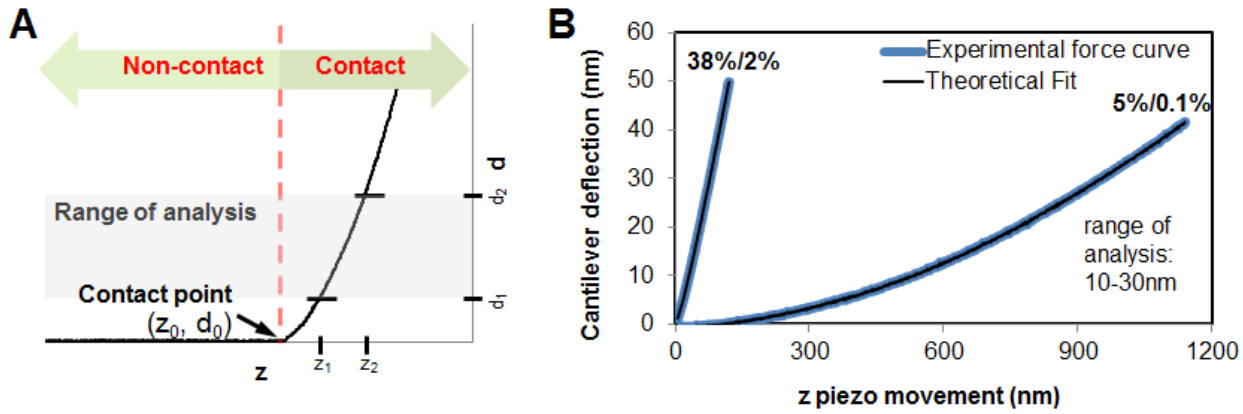

fig. S11. Mechanical characterization of PA gels. PA gels were mechanically characterized using AFM. **(A)** A typical AFM force curve and **(B)** representative force indentation profiles of two different PA gel variants are shown.

table S1. Elastic modulus of PA gels. Elastic modulus of a range of PA gels were determined using AFM. Errors reported as the standard deviation.

%Acrylamide/ %Bis-Acrylamide	**Elastic Modulus, *E* (kPa)**
5/0.10	3.70 ± 0.08
5/0.26	8.42 ± 1.11
10/0.3	44.2 ± 3.42
15/0.6	227 ± 23.4